

**AN INVESTIGATION OF NONLINEAR CONTROLLER FOR
PROPULSION CONTROLLED AIRCRAFT**

FINAL REPORT

(February 1, 1996 - January 31, 1997)

FINAL
IN-03-CR
0017
021794

**Research Supported by
NASA Dryden Flight Research Center
Cooperative Agreement NCC4-104**

NASA Dryden Investigator: John J. Burken

**Prepared by: Ping Lu
Department of Aerospace Engineering and Engineering Mechanics
Iowa State University
Ames, IA 50011-3231
February, 1997**

TABLE OF CONTENTS

1.	Background and Summary	1
2.	Nonlinearities in Propulsion Controlled Aircraft	3
3.	A Predictive Control Method	5
4.	Control of a Crippled Aircraft	9
4.1	Aircraft Model	9
4.2	Longitudinal Control	10
4.3	Controlled Turn	12
5.	PCA Tuck-Mode Controller for the C-17 Aircraft	13
5.1	Tuck-Mode of the C-17 Aircraft	13
5.2	Optimal PID Control Laws	14
5.3	Longitudinal Controller Design Procedure	16
6.	Conclusions	19
	References	20
	Figures	23-31

1. Background and Summary

Aircraft control systems are usually very reliable because of redundancy and multiple control surfaces. However, there are rare occasions when potentially disastrous flight control system failures do occur. At such times, the use of appropriate modulation of engine thrust to stabilize the aircraft may be the only chance of survival for the people aboard. In several cases where complete loss of control systems has occurred in multi-engine aircraft, pilots used propulsion system to regain limited control of the aircraft with various degrees of success (see [1]).

In order to evaluate the feasibility of using only engine thrust modulation for emergency backup flight control, the NASA Dryden Flight Research Center has been conducting a series of analytical studies and flight tests on several different types of aircraft in a propulsion controlled aircraft (PCA) program. Simulation studies have included B-720, B-727, MD-11, C-402, C-17, F-18, and F-15, and flight tests have included B-747, B-777, MD-11, T-39, Lear 24, F-18, F-15, T-38, and PA-30 (see [1]–[7]). One objective was to determine the degree of control available with manual manipulation (open-loop) of the engine throttles. Flight tests and simulations soon showed that a closed loop controller could improve the chances of making a safe runway landing (see [2]). The major work to date has concentrated on three aircraft (F-15, F-18, and the MD-11). Successful landings using PCA controllers were performed on the F-15 and MD-11 without the use of control surfaces.

During the course of the research, some unique challenges have been identified (see [6]). Compared to the conventional flight control surfaces, the engines are slow and have limited control effectiveness. Hence the ability of the system to promptly respond to aerodynamic changes is limited. Consequently, many nonlinear effects, which are easily accommodated by a conventional flight control system, become significant issues in the design of an effective controller when the engines are used as the only control effectors. A number of nonlinear behaviors observed during PCA flight tests, which are not meant to be exhaustive, are reviewed in the next section.

The flight controllers for the PCA thus far have been designed based on linearized models of the aircraft dynamics and the engines. Nonlinear simulation and flight testing are then carried out to tune the controller gains for enhanced performance. We realize, however, that an alternative is to recognize the nonlinearities in a PCA, and try to incorporate them as much as possible in the controller design. Such a controller is likely to be more responsive to the inherent nonlinearities in the system, and thus produces more effective control. This investigation represents a preliminary attempt in this direction, and part of the results have been reported in the pending article Ref. [8]. In particular, a recently developed nonlinear predictive control method is introduced as a potential design tool for the PCA controller. This approach bears some of the similar features that make the Linear Quadratic Regulator (LQR) method highly successful for linear systems. Thus it appears to be an appealing tool to be employed in the design of a nonlinear PCA controller. A problem of controlling a crippled aircraft is used to demonstrate the potential of this method in a highly demanding environment such as in PCA applications. In this problem, an airplane that lost the use of its rudder is controlled with reasonable satisfaction by including the nonlinear dynamic coupling effects in the control law design.

As an evolving step toward fully nonlinear PCA controller design, this research also carried out, in conjunction with a PCA project conducted in the summer of 1996 at Dryden, a PCA longitudinal controller design for the C-17 transport aircraft at a specific flight condition. At that condition the linearized PCA dynamics exhibits the so-called “Tuck-mode” behavior which in this case is an unstable mode. The controller that works for other flight conditions could not control the aircraft satisfactorily. A successful PCA controller was designed for the C-17 at this condition by an innovative two-step design process. First an optimal PID full-state feedback control law was designed to stabilize the aircraft. Then this PID control law was used as the starting point for iterative design of an output feedback controller using the Nonlinear Control Design (NCD) toolbox in the MATLAB.¹ Some of

¹MATLAB is a trade mark of the Mathworks Inc..

the details are given in Section 5.

2. Nonlinearities in Propulsion Controlled Aircraft

The flight control of the PCA is achieved by using differential thrust for lateral/directional control and symmetric thrust for longitudinal control. Refs. [2] and [4] give detailed account of this principle. Because of the limited control effects of the engines, however, a number of nonlinearities in the PCA which are otherwise insignificant when the aerodynamic control surfaces are operative become prominent. Some of the notable nonlinear phenomena in the PCA include:

1. Engine dynamics: Engine deceleration inputs usually reduce the thrust faster than engine acceleration inputs increase the thrust. The engines are slower to respond when the throttles are moved forward than when the throttles are moved back. Typically, a high bypass turbofan engine exhibits very slow thrust increase initially. Once the thrust reaches about 20% of the maximum thrust, the thrust response improves dramatically. The thrust decay shows similar nonlinear effects.
2. Engine saturation: Because of the limited control authority, the control commands can easily cause the engines to operate at their limits. For instance, a large roll command may cause one engine to saturate while the other engine still has more control authority available. This will lead to unsatisfactory lateral/directional control. Also, in low-speed landing approaches, the commanded engine thrust is close to idle. Disturbances caused by gusty conditions could result in engine saturation at the idle. Being a low bandwidth system, the engines may also experience rate saturation, and this is compounded by the nonlinear aspect of the thrust response.
3. Ram drag: Ram drag is due to the mass flow rate term which is a function of fan speed, nozzle area, exhaust temperature and other flight conditions. It affects the dynamics of the PCA and is inherently nonlinear.

4. Engine inlet location: This term is aircraft-dependent and has caused the F-15 to respond in a minimum-phase fashion; but the F-18 behaves with a nonminimum-phase like response depending on the aircraft flight condition. This could in fact be attributed to the nonlinear interactions between the airframe and propulsion system.
5. Dynamic cross-coupling: It has been observed that at high bank angles, the longitudinal control of the PCA deteriorates dramatically (see [6]). This is caused by the cross-coupling effects between the lateral and longitudinal dynamics of the PCA. Engine saturation can also contribute to the cross-coupling which in turn degrades both lateral and longitudinal control effectiveness. This degradation of performance results from the fact that the longitudinal control lateral control systems are usually designed separately based on decoupled linearized dynamics.

The flight test data of the F-18 System Research Vehicle (SRA) at the NASA Dryden Flight Research Center illustrates some of the above aspects. This F-18 SRA, as shown in Fig. 1, is a twin-engine, two-seat airplane. The aircraft is powered by two General Electric F404-GE-400 afterburning turbofan engines rated at approximately 16,000 lb static thrust at sea level. The F-18 features a midwing configuration with a wing-root leading-edge extension (LEX) that extends from the forward portion of the fuselage and blends into the wing.

The F-18 flight test studies were conducted with the normal control surfaces locked in a trimmed position and the throttles were given a step input. A series of open loop, pilot evaluation maneuvers were flown at a condition of 10,000 ft, $V=195$ knots, gear up, flaps at 30 deg., in the direct electric link (DEL) mode with gain override. This mode allowed the aircraft to be flown in a "true" open loop mode without any feedback parameters interacting with engine dynamic responses.

Figure 2 shows the response to a doublet input in the throttles, denoted by power lever angles (PLAs). The two PLAs are virtually the same, therefore produce changes in symmetric thrust which mostly influences the longitudinal motion. The pitch rate response in Fig. 2 (b) decreased first as the PLAs were increased, and then rose up in response to the PLA increase.

This would indicate a nonminimum-phase system if this occurred in a linear system. But as the example in Section 4 will demonstrate, this could be actually caused by the nonlinear PCA dynamics. In Fig. 2 (c) the roll rate showed unsymmetric response to the PLA input: when the PLAs were increased, the variation in the roll rate was slow and gentle; when the PLAs were decreased, however, the roll rate showed a sharp and large transient response. This is another indication of nonlinear dynamics of the PCA.

Figure 3 shows response of the F-18 to a different PLA doublet input. Since the PLAs in this case caused differential thrust for the two engines, the lateral/directional response was more visible (Fig. 3 (b)), in the roll rate in particular. The engine thrust of the PCA can be determined based on several quantities, including fan speed, exhaust gas temperature, airflow, discharge pressure and other parameters. The discharge pressures for the two engines in this case are shown in Fig. 3 (c). It is clear that the engine response were slower when the throttles were increased than when the throttles were decreased.

3. A Predictive Control Approach

So far the designs of the controllers for the PCA have been based on linearized aircraft and engine models, and linear control methods have been used. In view of the above noted significant nonlinear behaviors, it seems logical to expect that an appropriately designed nonlinear controller may take these nonlinearities into account in the control law, and thus offer improved performance for the PCA. Compared with the success of the linear control theory, the nonlinear control theory is still in an incomplete and less satisfactory state, although remarkable progress has been made in recent years, particularly in geometric control theory (see [9]) In the aerospace control community, the nonlinear method known as dynamic inversion (Ref. [10] and references therein), which is based on the input-output feedback linearization technique in geometric control theory, has been the focus of active research. But it is felt that dynamic inversion may not be an ideal method for PCA controller design because of two major concerns: (1) The control authority of the engines is rather limited.

This means that control and control-rate saturations can easily happen. And when they do, the control law based on dynamic inversion becomes invalid. (2) The engines, as the control effectors, have very complicated nonlinear dynamics, and considerable modeling uncertainties are bound to be present. Since the principle of dynamic inversion is canceling system nonlinearities by state-feedback, robustness could be an issue in the presence of such large uncertainties.

An alternative is a nonlinear predictive control method developed more recently (see [11, 12, 13, 14, 15]). The potential advantages of this approach in PCA application lie in that no stringent conditions on the system are required, and in the event of saturation, the control law remains applicable and the control efforts are distributed in an optimal fashion. In the following, the basic concept of this approach and some results are briefly reviewed.

Consider a multivariable nonlinear control system modeled by

$$\dot{x} = f(x) + G(x)u = f(x) + \sum_{i=1}^m g_i(x)u_i \quad (1)$$

$$y = c(x) \quad (2)$$

where the state is x , defined in a compact set $X \subset R^n$, and $y \in R^l$ is the output. A piecewise continuous input $u \in R^m$ is admissible if for all $t \geq 0$ it satisfies the condition

$$u(t) \in \Omega = \{u(t) \in R^m \mid L_i \leq u_i(t) \leq U_i, i = 1, \dots, m\} \quad (3)$$

where the bounds L_i and U_i are given, and can be state- and time-dependent if need be. The vector functions $f(x)$, $g_i(x)$, and $c(x)$ are sufficiently differentiable on X . Suppose that a desired output is specified by a sufficiently smooth l -dimensional vector function $y^*(t)$, $t \geq 0$. The requirement on $y^*(t)$ is that a corresponding state trajectory $x^*(t)$ and control function $u^*(t)$ exist with $x^*(t) \in X$ and $u^*(t) \in \Omega$ for all $t \geq 0$, such that $x^*(t)$ and $u^*(t)$ satisfy (1), and $y^*(t) = c(x^*(t))$. While the explicit knowledge of $x^*(t)$ and $u^*(t)$ is not needed for control law design, their existence ensures that the desired response is feasible.

The control problem is to design a control law $u = r(x, y^*, t) \in \Omega$ for all $t \geq 0$ such that for an arbitrary initial conditions of the system (1), denoted by $x_0 \in X_0 \subset X$, $y(t) \rightarrow y^*(t)$

as $t \rightarrow \infty$. Note that when $y = c(x) = x$ and $y^*(t) = x^*(t)$, the problem becomes a state-regulation problem.

At any $t \geq 0$, let γ_i be the relative degree of the i th ($1 \leq i \leq l$) output y_i at $x(t)$ (γ_i is then the number of differentiations needed on $y_i = c_i(x)$ until any components of $u(t)$ appear explicitly). The influence of the current control $u(t)$ on the system response at $t + h$ for a time increment $h > 0$ is predicted by expanding each $y_i(t + h)$ in a γ_i th order Taylor series

$$y(t + h) \approx y(t) + z(x(t), h) + W(x(t), h)u(t) \quad (4)$$

where each component of $z(x, h) = (z_1(x, h), \dots, z_l(x, h))^T$ is defined by

$$z_i = hL_f^0(c_i) + \frac{h^2}{2!}L_f^1(c_i) + \dots + \frac{h^{\gamma_i}}{\gamma_i!}L_f^{\gamma_i-1}(c_i), \quad i = 1, \dots, l \quad (5)$$

and the i th row of the $l \times m$ matrix W is

$$W_i = \left(\frac{h^{\gamma_i}}{\gamma_i!}L_{g_1}L_f^{\gamma_i-1}(x_i), \dots, \frac{h^{\gamma_i}}{\gamma_i!}L_{g_m}L_f^{\gamma_i-1}(x_i) \right), \quad i = 1, \dots, l. \quad (6)$$

In the above the notation of Lie derivatives has been used to simplify the representation of the partial derivatives. Similarly, expand each $y_i^*(t + h)$ in a γ_i th order Taylor series

$$y^*(t + h) \approx y^*(t) + d(t, h) \quad (7)$$

where the i th component of $d(t, h)$ is

$$d_i(t, h) = hy_i^*(t) + \frac{h^2}{2!}\ddot{y}_i^*(t) + \dots + \frac{h^{\gamma_i}}{\gamma_i!}y_i^{*(\gamma_i)}(t), \quad i = 1, \dots, l \quad (8)$$

The tracking error at the next instant $t + h$ is then predicted as a function of $u(t)$ by

$$e(t + h) = y(t + h) - y^*(t + h) \approx e(t) + z(x(t), h) - d(t, h) + W(x(t), u(t), h). \quad (9)$$

The control $u(t)$ is then found by solving the constrained optimization problem

$$\min_{u(t) \in \Omega} J = \frac{1}{2}e^T(t + h)Qe(t + h) + \frac{1}{2}u(t)^TRu(t) \quad (10)$$

where Q and R are positive semidefinite matrices of appropriate dimensions. Define a vector saturater $s(\cdot) : R^m \rightarrow R^m$ by

$$s_i(q) = \begin{cases} U_i, & q_i \geq U_i \\ q_i, & L_i < q_i < U_i, \quad i = 1, 2, \dots, m \\ L_i, & q_i \leq L_i \end{cases} \quad (11)$$

for any $q \in R^m$. The results regarding the optimal control are summarized in the following [11, 12, 13]:

Replace $e(t+h)$ in (10) by the prediction (9). Suppose that the $m \times m$ matrix $P(x(t), h) = \{p_{ij}\} = W^T(x(t), h)QW(x(t), h) + R$ is nonsingular at $x(t)$. Then, for any $h > 0$, we have

1. *The unique optimal control $u_{op}(t)$ exists and is the unique solution of the equation*

$$u = s \left\{ \beta W^T Q (d - z - e) - [\beta (W^T Q W + R) - I] u \right\} \triangleq \rho(u) \quad (12)$$

where all the quantities are evaluated at t , I is an identity matrix, and

$$\beta = \left\{ \sum_{i=1}^m \sum_{j=1}^m p_{ij}^2 \right\}^{-1/2}. \quad (13)$$

2. *In general the fixed-point iteration sequence $\{u^k\}$ generated by*

$$u^k = \rho(u^{k-1}), \quad k = 1, 2, \dots, \quad \forall u^0 \in R^m \quad (14)$$

converges to $u_{op}(t)$ globally.

3. *When none of the components of $u_{op}(t)$ are on the boundary of the control set Ω , the closed-form control law from Eq. (12) is*

$$u = (W^T Q W + R)^{-1} [W^T Q (d - z - e)]. \quad (15)$$

An alternative formulation of the problem can be found in Ref. [14]. Discussions on closed-loop stability for several classes of systems under control law (15) and robustness of the controller are given in Ref. [12].

The optimal control command at any $t \geq 0$ is given by (12) which can be generated by the globally rapidly convergent algorithm (14), and this fixed-point algorithm is particularly suited for computer implementation. Even in the presence of control saturation, the $u(t)$ from the solution of (12) is still optimal in the sense of minimizing the performance index (10). When both control and control-rate are bounded, a minor modification in the saturator s used in the optimal control law will guarantee strict satisfaction of all the constraints (see [15]). When no control saturation is encountered, control law (12) simply reduces to the explicit closed form (15). For the PCA control application, this predictive control method may prove to be advantageous in this environment with severely limited control-authority and significant nonlinearities.

4. Control of a Crippled Aircraft

4.1 Aircraft Model

This example is used to demonstrate the application of the predictive control approach, and to illustrate that non-intuitive results may be achieved when the system nonlinearity is appropriately taken into account. Consider the following aircraft model which is the same as “aircraft A” in Ref. [16]:

$$\dot{\alpha} = -2.9998\alpha + q - \beta p \quad (16)$$

$$\dot{\beta} = -0.05586\beta - r + \alpha p \quad (17)$$

$$\dot{p} = -202.96\beta - 39.97p + 2.7943r - 0.70574qr - 601.37\delta_a \quad (18)$$

$$\dot{q} = -22.692\alpha - 4.0556q + 0.71992\beta p + 0.95965pr - 61.129\delta_e \quad (19)$$

$$\dot{r} = 6.8294\beta - 0.47937r - 0.78674pq \quad (20)$$

where the standard notation is used: α is the angle of attack (deg), β sideslip angle (deg), p roll rate (deg/sec), q pitch rate (deg/sec), and r the yaw rate (deg/sec). The two controls are aileron deflection δ_a (deg) and elevator deflection δ_e (deg).

This is a nonlinear model with cross-product terms retained, although the control effectors are still the conventional control surfaces. Nonetheless, some of the features this model presents are quite unconventional because of the nonlinearities, and the notable absence of the rudder may be conveniently interpreted as the loss of a control surface (rudder). Hence the difficulties in controlling this crippled aircraft resemble to some extent those which would be encountered in a PCA.

First of all, it can be easily shown that the linearized system to Eqs. (16-20) is not controllable (the controllability matrix only has rank 3) because the rudder is not available for control purpose. So pole-placement or LQR type of techniques for linear controller design are not applicable even for the linearized system. In fact, in the linearized system, Eqs. (17) and (20) constitute a free stable subsystem in β and r which is not influenced by any controls and other variables.² Secondly, the dynamic inversion approach for nonlinear controller design cannot be used for longitudinal control purpose if the usual coordinated flight (in which $\beta = 0$) is desired. This is because with the two controlled longitudinal outputs $y_1 = \alpha$ and $y_2 = q$, it can be readily verified that the nonlinear system does not have a relative degree (see [9]) whenever $\beta = 0$.

Since the predictive control method does not require any stringent conditions on the system, it appears that this approach is an attractive alternative for flight control design for this model of a “crippled” aircraft. We shall consider two control problems in the following. The first one demonstrates the effectiveness of the predictive control method, and the second shows that the controller based on the nonlinear dynamics can control the aircraft to achieve commanded turning maneuver, which would be impossible to do with only the linearized model.

4.2 Longitudinal Control

Suppose that the objective is to design a controller to track commands to the longitudinal motion while the lateral/directional motion is stabilized at $\beta = p = r = 0$, assuming full-

²This subsystem is nonetheless stable with a light damping of $\zeta = 0.1$ and a time constant of 3.9 sec.

state feedback. More specifically, suppose that the aircraft is to be controlled to achieve the quasi-trim conditions

$$\alpha^* = \alpha_{com}, \quad q^* = q_{com}, \quad \beta^* = p^* = r^* = 0 \quad (21)$$

where the commanded constants α_{com} and q_{com} satisfy the relationship

$$\alpha_{com} = 0.333355557q_{com}. \quad (22)$$

This relationship is obtained from setting $\dot{\alpha} = 0$. Use the values in Eq. (21) as the reference trajectory for a full-state regulation problem ($y = c(x) = x$ in Eq. (2)). The predictive control approach introduced in the preceding section is then employed to design a nonlinear controller. The closed-form control law follows directly from Eq. (15). The controller parameters are selected to be $Q = \text{diag}\{Q_1, \dots, Q_5\}$, and $R = \text{diag}\{R_1, R_2\}$ with

$$Q_1 = 1.0, \quad Q_2 = 0.1, \quad Q_3 = 1.0, \quad Q_4 = 1.0, \quad Q_5 = 0.1, \quad R_1 = 0.1, \quad R_2 = 0.1. \quad (23)$$

The value of $h = 0.4$ is also used. It was found that in this case the system performance was insensitive to the choices of R_1 and R_2 . Any values of R_1 and R_2 in the range of $[0, 10]$ would give practically the same response. On the other hand, the choices of Q_i seem to have more profound influence on the response and stability. A satisfactory set of Q_i , however, are not difficult to determine by numerical simulations, because these parameters have a similar interpretation and effect as the weightings in an LQR problem.

Figure 4 shows the time histories of the states for the initial conditions

$$\alpha(0) = q(0) = 0, \quad \beta(0) = 5 \text{ (deg)}, \quad p(0) = 5 \text{ (deg/sec)}, \quad r(0) = -5 \text{ (deg/sec)}$$

and command inputs

$$\alpha_{com} = 1.67 \text{ (deg)}, \quad q_{com} = 5 \text{ (deg/sec)}.$$

Figure 5 presents the corresponding control histories. It can be seen that all the lateral/directional variables subside to zero in about 3 seconds, despite the nonzero initial conditions. The longitudinal motion tracks the commanded α_{com} and q_{com} gracefully in

about 1.2 second. The local closed-loop stability of the nonlinear system is checked by examining the eigenvalues of the linearized system.

It is interesting to observe the time-history of $\alpha(t)$ in Fig. 4. The initial movement of $\alpha(t)$ is opposite to the commanded direction. This would indicate a nonminimum-phase system if this phenomenon occurs in the response of a linear system. However, it can be shown that the linearized system in this case is actually minimum-phase with all the transmission zeros in the left open half of the complex plane. The undershoot of $\alpha(t)$ is caused by a nonlinearity in the system, the cross-product term βp in particular in Eq. (16). Another point is that when the predictive controller is constructed based on the linearized dynamics, although the linear system is stable, the nonlinear system is not when the controller is applied to the nonlinear dynamic equations. Figure 6 shows the state histories of the nonlinear system with the linear controller. It is evident that the motion entered a limit cycle.

The above phenomena clearly indicate that the analysis and controller design based on the linearized model in this case are inadequate.

4.3 Controlled Turn

Suppose now that the aircraft is to be controlled to achieve a steady-state turn in which all the state variables are constant with $r = r_{com}$. This can be a difficult maneuver for this crippled aircraft because the rudder, which is missing, is the primary control surface for yaw control. Indeed, if only the linearized dynamics are considered by ignoring the nonlinear terms in the dynamic equations, any commanded turn is impossible to achieve for any $r_{com} \neq 0$, since the β - r subsystem is not influenced by any controls and other states in the linearized system. However, when the nonlinearity is retained, this turning maneuver is actually feasible because of the cross coupling. For instance, for $r_{com} = 5$ (deg/s), such a quasi-trim condition is defined by

$$\alpha^* = 4 \text{ (deg)}, q^* = 15.39 \text{ (deg/s)}, \beta^* = 2.63 \text{ (deg)}, p^* = 1.28 \text{ (deg/s)}, r^* = 5 \text{ (deg/s)}. \quad (24)$$

Use the values in above equation to specify the reference trajectory and the same predictive

controller designed for the above pitch control maneuver is employed for flight control. For the initial conditions

$$\alpha(0) = \beta(0) = p(0) = q(0) = r(0) = 0.$$

Figs. 7 and 8 show the histories of the state variables and two controls δ_a and δ_e . It can be seen that the controller effectively drives all the states to their trim values in about 3 seconds.

This example essentially demonstrates the effect of the second-order terms in the aircraft dynamics which are ignored in the linearized model. Just as in stability analysis, the influence of higher-order terms becomes crucial when the first-order effects diminish. Since the symmetric thrust modulation of the PCA generates pitch moment variation and differential thrust change produces yaw moment variation, but no direct roll control is provided, the PCA would in this aspect resemble a crippled aircraft that loses the use of its aileron which provides the primary roll control. In this sense, the above exercise illustrates that when the cross-coupling nonlinearity in the system is appropriately taken into account in the controller design, it may actually renders the PCA more controllable.

5. PCA Tuck-Mode Controller for the C-17 Aircraft

5.1 Tuck-Mode of the C-17 Aircraft

The C-17 is a heavy military transport aircraft and has four engines. A study was conducted in 1996 at the McDonnell Douglas Aircraft Company and NASA Dryden on engine-only flight control for the C-17. The study found that in most flight conditions the PCA controller can control the aircraft reasonably well. But at one particular condition specified by Mach 0.7, $h = 30,000$ ft, weight=576,000 lb, and zero flap, the longitudinal PCA controller failed to control the climb rate (or equivalently the flight path angle) to track \dot{h} -commands. A closer examination of the linearized PCA model reveals that the C-17 longitudinal dynamics at that condition have the so-called “tuck mode” [17]. This is the case when the phugoid mode degenerates into two real first-order modes, one of which is

unstable. Furthermore, the dynamics from the engine thrust to flight path angle at that condition are nonminimum-phase. In addition, it turns out that a singularity exists in this case in the system dynamics so that the conventional nonzero set-point tracking control design is not applicable (see next section). All these, in conjunction with the usual limited control effectiveness of thrust on aircraft attitude, render the controller design problem a challenging one. Part of the effort in this research was devoted to this problem. A satisfactory PCA controller was designed to provide accurate longitudinal control. Perhaps more importantly, the methodology used in this exercise, which combines the well-developed state-space techniques and state-of-the-art control design tools, may prove to be equally valuable in other applications.

5.2 Optimal PID Control Laws

In this section we briefly review an approach for design of optimal PID, full-state feedback controllers by an LQR method [18]. Given a linear system

$$\dot{x} = Ax + Bu \quad (25)$$

$$y = Cx \quad (26)$$

where $x \in R^n$, $u \in R^r$, $y \in R^m$, and $m \leq r \leq n$. A nonzero set point $z \in R^m$ is given for the system. This means that there exist a pair of constant steady-state $\{x_s, u_s\}$ such that x_s and u_s satisfy $Ax_s + Bu_s = 0$ and $y_s = Cx_s = z$. To design a PID control law for y to asymptotically track z , Parker proposed the following technique [18]: Define a new state vector $\xi = (y^T \eta^T)^T = Tx$, where $\eta \in R^{n-m}$ and $\eta = Lx$ for some $(n-m) \times n$ matrix L . The selection of L should make the transformation matrix

$$T = \begin{pmatrix} C \\ L \end{pmatrix} \quad (27)$$

nonsingular (which automatically requires C to be of full row rank). Then,

$$\dot{\xi} = TAT^{-1}\xi + TBu \triangleq F\xi + Gu \quad (28)$$

Next, introduce the augmented state $\theta = (\theta_1^T \ \theta_2^T \ \theta_3^T)^T \in R^{n+m}$, where

$$\theta_1 = e = z - y, \quad \theta_2 = \dot{e}, \quad \theta_3 = \dot{\eta} \quad (29)$$

and the new control $v = \dot{u}$. The augmented state equations are then

$$\dot{\theta} = \Phi\theta + \Gamma v \quad (30)$$

where the matrices Φ and Γ can be easily obtained from the definition of θ and (28). Now the following LQR problem is solved where the performance index

$$J = \frac{1}{2} \int_0^\infty (\theta^T Q \theta + v^T R v) dt \quad (31)$$

is minimized. The optimal solution is given by

$$\dot{u} = v = -R^{-1} \Gamma^T P \theta = K_1 \theta_1 + K_2 \theta_2 + K_3 \theta_3 \quad (32)$$

where P is the solution of the standard algebraic Riccati equation associated with (30) and (31). Integrating (32) once yields a control law

$$u(t) = K_1 \int_0^t e(\tau) d\tau + K_2 e(t) + K_3 \eta(t) \quad (33)$$

If η is selected in such a way that it contains the first-order derivative of y , this is a PID feedback control law.

Remarks:

1. Although not mentioned explicitly in Ref. [18], the controllability of the augmented system (30) is obviously required for the unique positive definite solution of the associated algebraic Riccati equation.
2. Again, although not discussed in Ref. [18], the closed-loop system stability under this control law can be intuitively seen from how the control law is derived. The minimization of the performance index (31) ensures that $\theta \rightarrow 0$. By the definition of θ , this leads to $e \rightarrow 0$ ($y = z$) and $\eta \rightarrow \eta_s$ where η_s is some constant vector. Since $\eta = Lx$ and $y = Cx$, the steady-state value of x is obtained from $x_s = T^{-1}(z^T \ \eta_s^T)^T$, which is necessarily finite.

5.3 Longitudinal Controller Design Procedure

The complete 10-state, 6-DOF system equation for the C-17 includes some coupling between the longitudinal and lateral/directional dynamics. To simplify the preliminary design, we shall at first ignore these coupling effects and the engine dynamics (which now are the actuator dynamics). Therefore the first-cut design of the controller is based on the 5-state longitudinal dynamics

$$\dot{x}_{lon} = A_{lon}x_{lon} + B_{lon}u \quad (34)$$

$$y = C_{lon}x_{lon} \quad (35)$$

with $x_{lon} = (\theta \ q \ \alpha \ v \ h)^T$ and $y = \dot{h} = V_0(\theta - \alpha)$, where the standard notation is used, i.e., θ denotes the pitch angle, q the body pitch rate, α the angle of attack, v the velocity, and h the altitude. The control is the engine throttle input.

Aside from the tuck-mode and the nonminimum-phase behavior, this model also poses a special challenge for the tracking controller design: the conventional optimal nonzero set point tracking control law [19] does not exist because the matrix $C_{lon}A_{lon}^{-1}B_{lon}$, the inverse of which is required for the control law, is singular. In addition, it is desired to include an integrator in the controller to enhance the tracking performance, particularly in the presence of possible system parameter uncertainties. Finally, the controller should use available measured feedback signals instead of requiring state feedback.

The controller design was accomplished in two steps. First, the approach introduced in the preceding section was applied to the simplified longitudinal dynamics (34). The problem is posed as a tracking problem in which a constant \dot{h}_{com} is to be tracked by the output $y = \dot{h}$. It should be pointed out that because of the dependence of the longitudinal dynamics on the altitude h , $\dot{h} = \text{constant}$ is not exactly a set (trim) point of the C-17 with engine-only control. Also, although the system (34) is not strictly uncontrollable, its controllability matrix is nearly singular. This renders the solution of the algebraic Riccati equation inaccurate. When combined with the ignored coupling between the longitudinal and lateral dynamics and the engine dynamics, the resulting PID controller will not be

able to exactly control \dot{h} to track \dot{h}_{com} . Nonetheless, the method described in the preceding section is systematic and easy to use. The outcome then serves as a starting point for further iterations in the controller design.

Next, the controller obtained in the first step was applied to the complete 10-state system model with all the first-order engine dynamics and control rate-limiters included. The controller parameters were then further tuned by using the MATLAB Nonlinear Control Design (NCD) toolbox. The NCD toolbox allows the user to specify the desired shape of the response of a system with a graphic interface. The user-specified parameters of the system (which can be nonlinear) are then repeatedly adjusted by a sequential quadratic programming algorithm until the actual response of the system matches the desired one. Step response was used in the C-17 PCA controller design. As in any method based on numerical optimization, the initial values of the optimization parameters can be very important to the final success of the method. This is where the baseline design obtained in the first step fits in.

Finally, the controller is switched from a state feedback controller obtained above to an output-feedback controller. At this point, the feedback signals to the controller, are x_{lon} and the controlled variable \dot{h} , and the control law takes the form of

$$u = k_p(\dot{h}_{com} - \dot{h}) + k_i \int_0^t (\dot{h}_{com} - \dot{h}) d\tau + K_x^T x_{lon} \quad (36)$$

where $K_x \in R^5$. Among them, the measurement of the angle-of-attack α is usually quite noisy. So the normal acceleration a_z (ft/s²) measured at the Inertial Reference Unit (IRU) was used in place of α . The reason for using a_z is that a_z is approximately $\ddot{h} = d(\dot{h} - \dot{h}_{com})/dt$. Hence it provides the derivative information of the controlled variable \dot{h} in the control law (the D-term in the PID control law). Let $w = (\theta \ q \ v \ h \ a_z)^T$. Then a linear transformation $w = Hx_{lon}$ exists, where the last row of the H matrix comes from the linearized relationship between a_z and x_{lon} . The new gain vector with w as the feedback signal is simply $K_w = H^{-1}K_x$. Finally, the dependence of the control law on h stems from the weak dependence of the longitudinal dynamics on h . For the purpose of controlling \dot{h} the h -feedback is not

necessary or desired. For instance, for an extended climb/descent, the magnitude of the h -feedback term will become larger and larger, and could eventually saturate the controller. To eliminate the h -feedback requirement, the corresponding component in K_w was set to zero. The remaining gains, including k_p and k_i , were then fine tuned by using the NCD toolbox again to compensate for this final adjustment. The final output-feedback PCA controller takes the form of

$$u = k_p(\dot{h}_{com} - \dot{h}) + k_i \int_0^t (\dot{h}_{com} - \dot{h}) d\tau + k_\theta \theta + k_q q + k_v v + k_{a_z} a_z \quad (37)$$

Figure 9 depicts the controller configuration. Figure 10 show the response of the climb rate \dot{h} to a 5 ft/sec command input. Both the transient and steady-state responses appear to be quite good. Notice the initial dip in the \dot{h} history, which indicates a nonminimum-phase system. Figure 11 plots the corresponding engine command, which is not excessive.

Remarks:

1. The principle of the above design procedure can be applied to other cases. Standard LQR-based control design methods are systematic, easy to apply, and can yield very satisfactory performance. But they inevitably produce full-state feedback control laws which may not be realistic. On the other hand, the design of output-feedback controllers heavily depends on trial and error, and laborious numerical iterative processes are usually involved [20]. Empirical methods also exist for tuning of classical PID controllers. But for MIMO systems their applicability and effectiveness are severely limited. The design approach used here suggests that a different route may be taken. In this approach an appropriate LQR-based method is first applied, possibly to a simplified but essential part of the complete dynamics. Once a baseline controller is obtained, it is added to the complete system model with actuator dynamics included. Then a state-of-the-art interactive graphic tools for control design, such as the NCD toolbox, is employed to tune the controller parameters. At this stage, appropriate measured outputs replace the unavailable state variables, and nonessential feedback paths are removed. The finally obtained controller should meet the design objectives.

2. It is recognized that this procedure does not automatically guarantee a success, and engineering judgments are still important in the process. But past experience [21] and the current exercise have indicated that this approach can significantly reduce the effort and time consumed in the intensive trial-and-error design iterations, and the controllers so obtained are usually quite satisfactory.

6. Conclusions

In this research the nonlinear phenomena observed in previous PCA flight testing were examined and analyzed. The predominant nonlinearities come from the engine dynamics, interactions between propulsion system and the airframe, and the dynamic cross-coupling effects between longitudinal and lateral-directional motions. It is concluded that if in the design of the PCA controller the essential aspects of these nonlinearities are incorporated, it is likely that the performance of the PCA controller can be markedly enhanced to give more accurate flight control of the aircraft. A nonlinear predictive control method is introduced as a potential approach for design of such a nonlinear PCA controller. The problem of controlling a crippled aircraft, which from a control point of view bears some similarity with PCA, is solved to demonstrate that higher level of control effectiveness can be achieved when the system nonlinearities are included in the controller.

As a part of the effort in this research and in conjunction with a PCA project conducted in the summer of 1996 at Dryden, a PCA longitudinal controller design for the C-17 transport aircraft was designed. In this process, although the PCA model was still linear, several attempts by using conventional linear control methods failed because of the particular dynamic behavior of the aircraft at that flight condition. A methodology was developed that combines state-space based optimal PID control law design approach and interactive numerical design approach facilitated by the Nonlinear Control Toolbox in MATLAB. A successful controller was obtained for the C-17, and the methodology itself may prove to be a valuable addition to the existing design techniques.

References

- [1] Burcham F. W., Jr., Trindel Maine, John J. Burken and Drew Pappas, "Flight Test of an Emergency Flight Control System using Only Engine Thrust on an MD-11 Transport Airplane", to appear in the *Proceedings of the AIAA Guidance, Navigation, and Control Conference*, July, 1996, San Diego, CA.
- [2] Burcham, F. W. Jr., and Fullerton, C. G., "Controlling Crippled Aircraft—With Throttles", NASA TM-104238, Sept., 1991.
- [3] Gilyard, G. B., Conley, J. L., Le, J., and Burcham, F. W. Jr., "A Simulation Evaluation of a Four-Engine Jet Transport Using Engine Thrust Modulation for Flight-path Control", AIAA paper 91-2223, also NASA TM-4324, 1991.
- [4] Burcham, F. W. Jr., Maine, T. A., and Wolf, T., "Flight Testing and Simulation of an F-15 Airplane Using Throttles for Flight Control", NASA TM-104255, August, 1992.
- [5] Burcham, F. W. Jr., Maine, T. A., Fullerton, C. G., and Wells, E. A., "Preliminary Flight Results of a Fly-by-Throttle Emergence Flight Control System on an F-15 Airplane," NASA TM 4503, 1993.
- [6] Maine, T., Burken, J., Burcham, F., and Schaefer, P., "Design Challenges Encountered in a Propulsion-Controlled Aircraft Flight Test Program", AIAA paper 94-3359, *30th AIAA/ASME/SAE/ASEE Joint Propulsion Conference*, June 27-29, 1994, Indianapolis, IN.
- [7] Burken, J. J., Burcham, F. W. Jr., Feather, J., Kahler, J., Maine, T., and Goldthorpe, S., "Flight Test of a Propulsion Based, Low Bandwidth Emergency Flight Control System on the MD-11 Aircraft", *The AIAA Guidance, Navigation, and Control Conference*, July 29–31, 1996, San Diego, CA.

- [8] Lu, P., and Burken, J. J., "Propulsion Controlled Aircraft: a Nonlinear Perspective," *First International Conference on Nonlinear Problems in Aviation and Aerospace*, Daytona Beach, FL, May 9–11, 1996. A revised version is accepted for publication in the *Nonlinear World*, 1997.
- [9] Isidori, A. *Nonlinear Control Systems: An Introduction*, 2nd Edition, Springer-Verlag, New York, 1989.
- [10] Enns, D., Bugajski, D., Hendrick, R., and Stein G., "Dynamic Inversion: an Evolving Methodology for Flight Control Design," *International Journal of Control*, Vol. 59, No. 1, 1994, pp. 71–91.
- [11] Lu, P. "Nonlinear Predictive Controllers for Continuous Systems." *Journal of Guidance, Control, and Dynamics*, **17**, 553–560, 1994.
- [12] Lu, P. "Optimal Predictive Control of Continuous Nonlinear Systems." *International Journal of Control*, **62**, No. 3, 633–649, 1995.
- [13] Lu, P. "Constrained Tracking Control of Nonlinear Systems." *Systems & Control Letters*, **27**, 305–314, 1996.
- [14] Singh, S. N., Steinberg, M., and DiGirolamo, R. D. "Nonlinear Predictive Control of Feedback Linearizable Systems and Flight Control System Design." *Journal of Guidance, Control, and Dynamics*, **18**, No. 5, 1023–1028, 1995.
- [15] Lu, P., "Tracking Control of Nonlinear Systems with Bounded Controls and Control Rates." *The 13th International Federation of Automatic Control World Congress*, June 30–July 5, 1996, San Francisco, CA.
- [16] Cochran Jr., J. E., and Ho, C.-S., "Stability of Aircraft Motion in Critical Cases", *Journal of Guidance, Control, and Dynamics*, **6**, No. 4, 272–279, 1983.

- [17] McRuer, D., Askensas, I., and Graham, D., *Aircraft Dynamics and Automatic Control*, Princeton University Press, 1973.
- [18] Parker, K. T., “Design of Proportional-Integral Derivative Controllers by the Use of Optimal-Linear-Regulator Theory”, *Proceedings of IEE*, Vol. 119, No. 7, July, 1972, pp. 911–914.
- [19] Kwakernaak, H., and Sivan, R., *Linear Optimal Control Systems*, Wiley-Interscience, New York, 1972.
- [20] Stevens, B. L., and Lewis, F. L., *Aircraft Control and Simulation*, Wiley-Interscience, New York, 1992.
- [21] Burken, J., Maine, T., Burcham, F., and Kahler, J., “Longitudinal Emergence Control System Using Thrust Modulation Demonstrated on an MD-11 Airplane”, AIAA 96-3062, 32nd AIAA/ASME/SAE/ASEE Joint Propulsion Conference, July 1-3, 1996, Lake Buena Vista, FL.

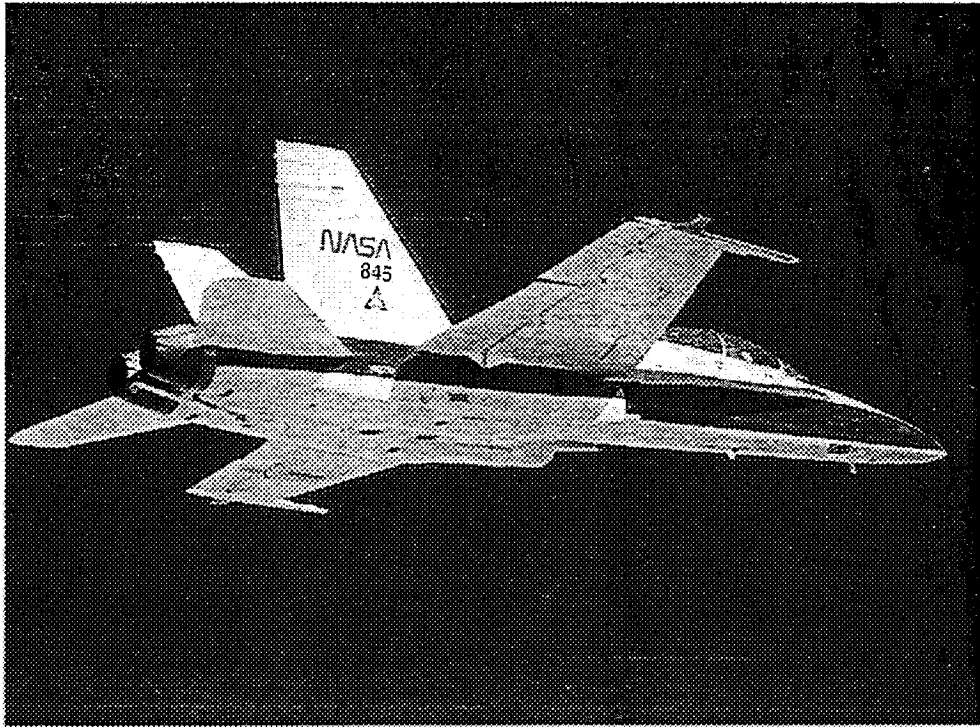


Figure 1: NASA F-18 System Research Vehicle

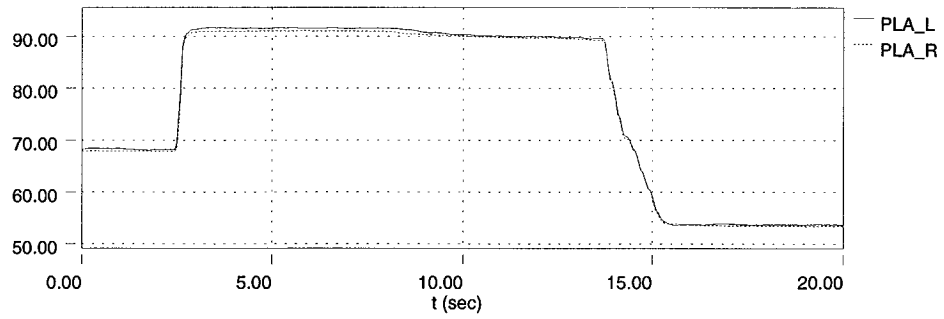


Fig. 2 (a): Power lever angle for the left engine, PLA_L (deg) and for the right engine, PLA_R (deg)

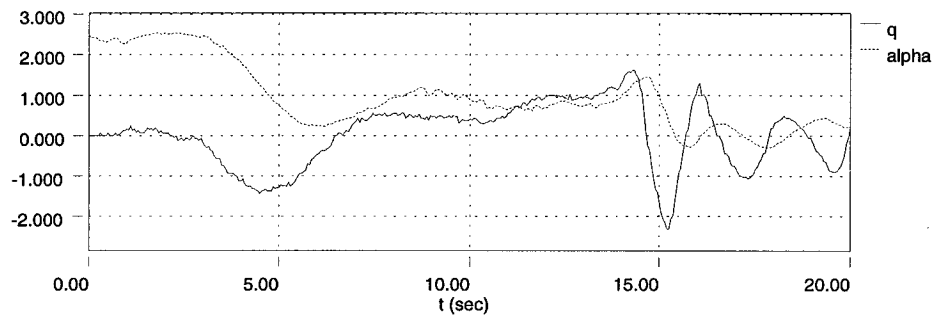


Fig. 2 (b): Responses of pitch rate q (deg/s) and angle of attack α (deg)

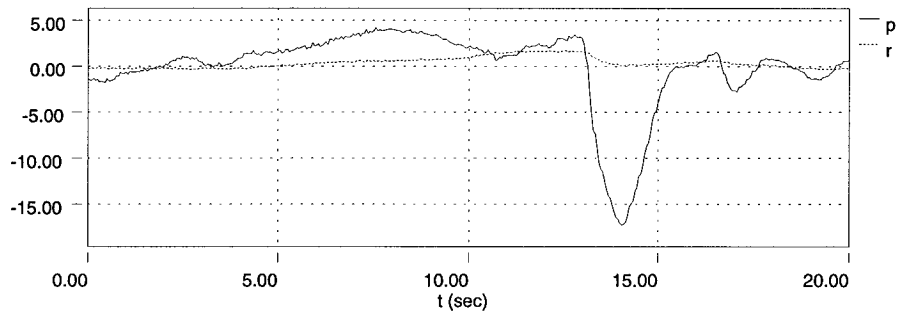


Fig. 2 (c): Responses of roll rate p (deg/s) and yaw rate r (deg/s)

Figure 2: F-18 flight test I

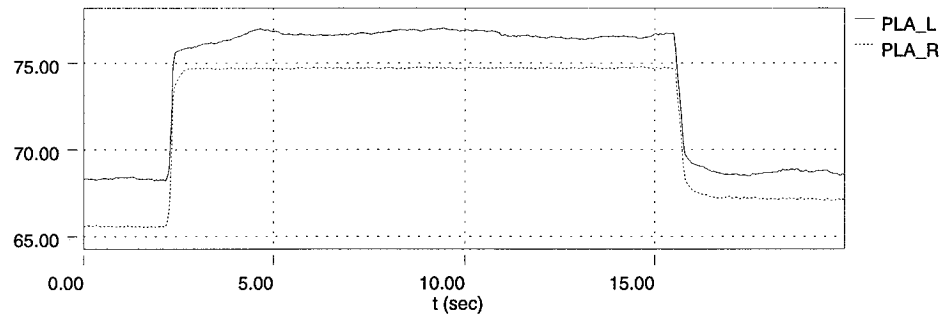


Fig. 3 (a): Power lever angle for the left engine, PLA_L (deg) and for the right engine, PLA_R (deg)

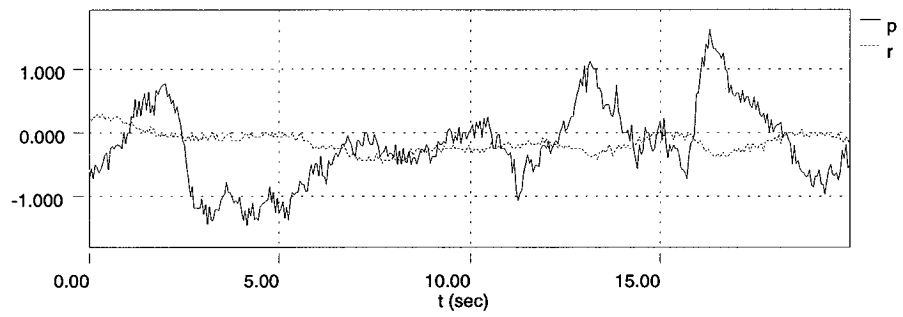


Fig. 3 (b): Responses of roll rate p (deg/s) and yaw rate r (deg/s)

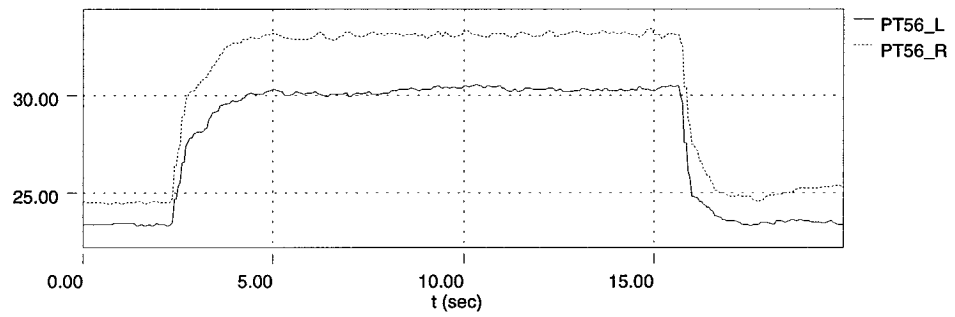


Fig. 3 (c): Discharge pressure for the left engine PT56_L (psf) and for the right engine PT56_R (psf)

Fig. 3: F-18 flight test II

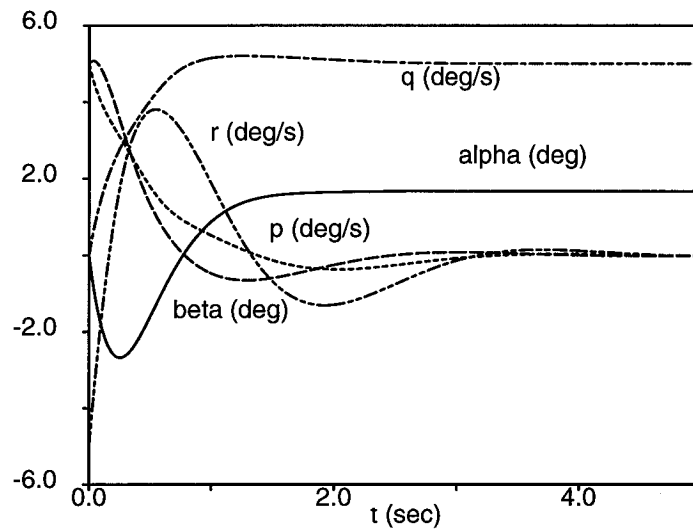


Fig. 4: State histories of the aircraft for the longitudinal maneuver

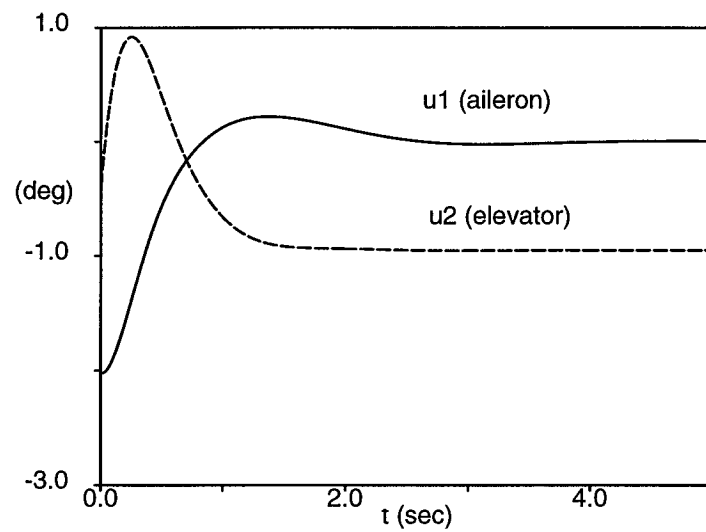


Fig. 5: Control surface deflections for the longitudinal maneuver

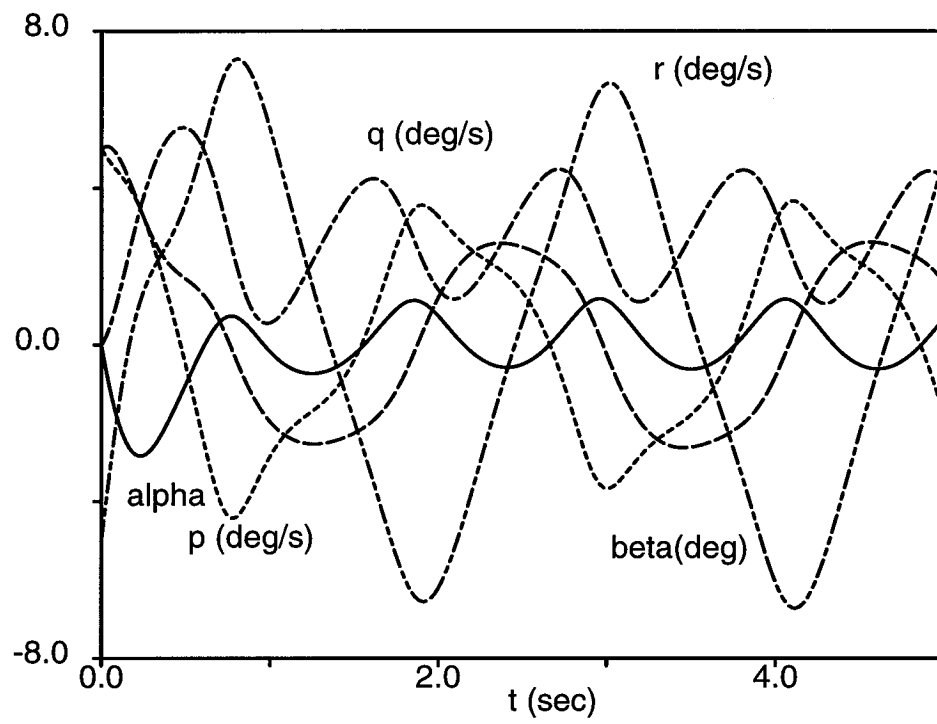


Fig. 6: State histories when the linear controller applied to the nonlinear aircraft dynamics

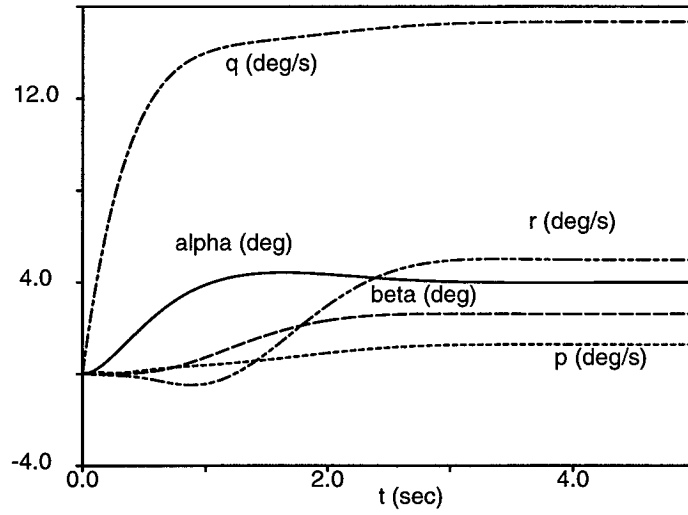


Fig. 7: State histories for the turning maneuver

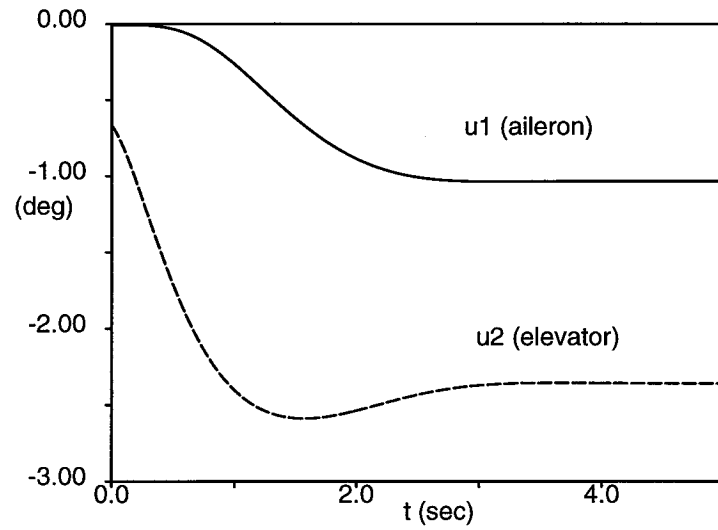


Fig. 8: Control surface deflections for the turning maneuver

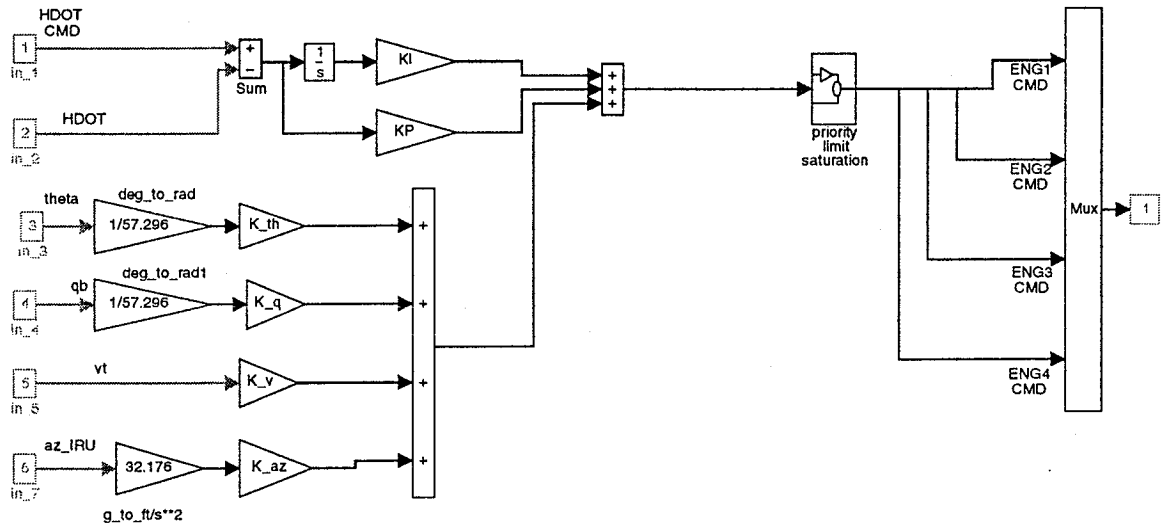


Fig. 9: C-17 Longitudinal PCA Controller

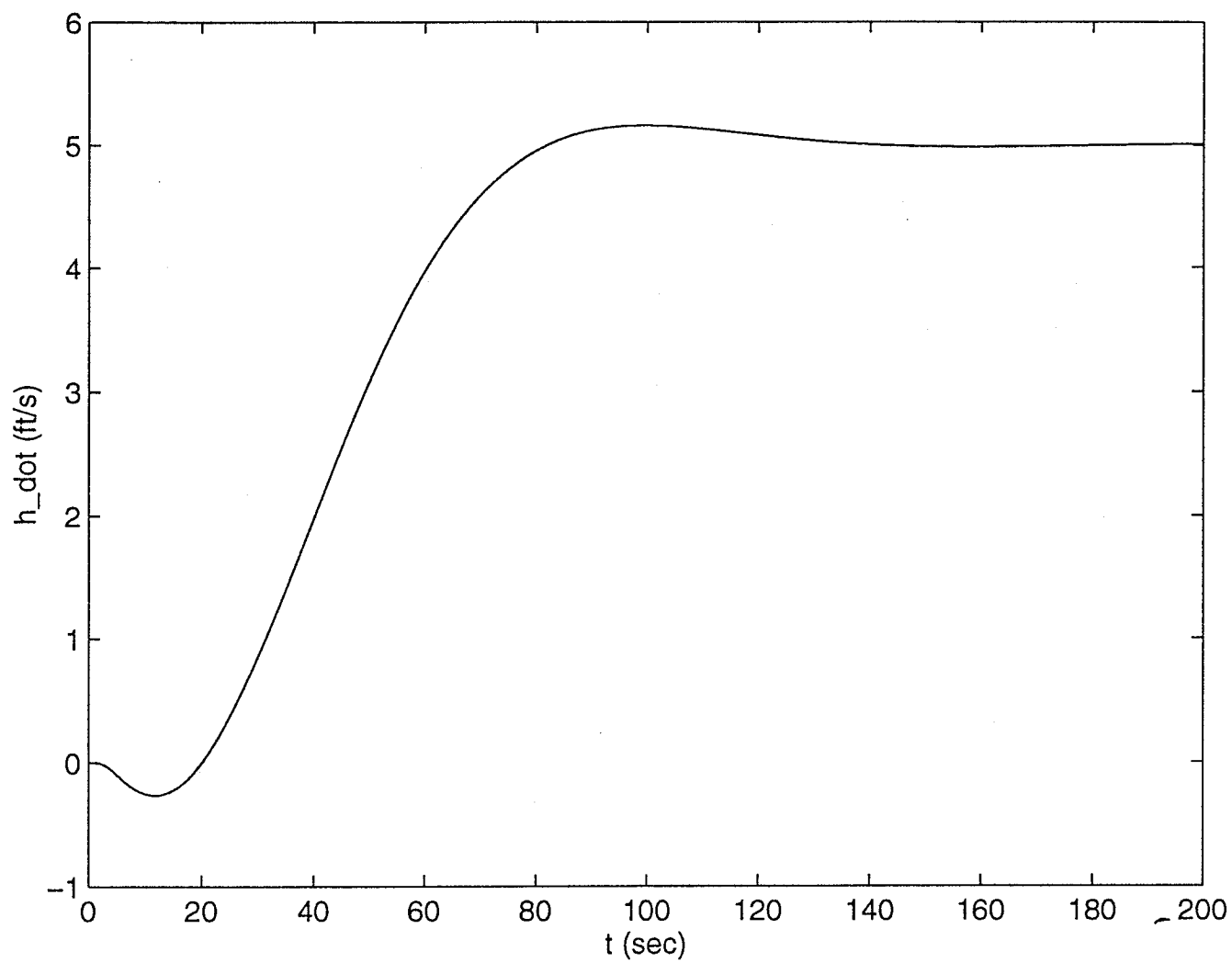


Fig. 10: Step response of the climb rate of the C-17 (command input = 5 ft/sec)

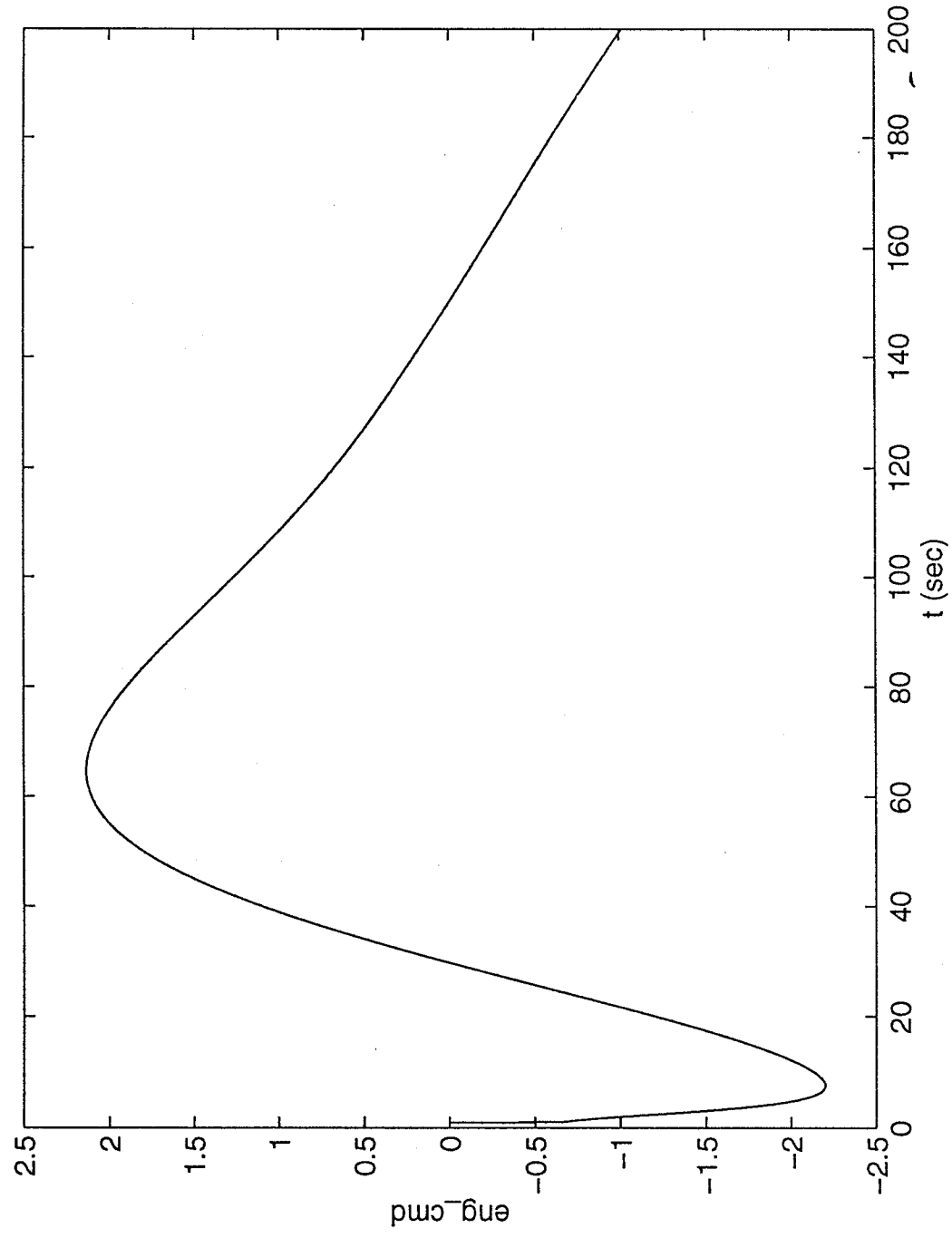


Fig. 11: C-17 engine throttle input corresponding to a commanded climb rate input of 5 ft/sec